Dye Adsorption and Decomposition on Two-Dimensional Titanium Carbide in Aqueous Media

ARTICLE · JULY 2014

DOI: 10.1039/C4TA02638A

6 AUTHORS, INCLUDING:

Olha Mashtalir
Drexel University
20 PUBLICATIONS **547** CITATIONS
SEE PROFILE

Kevin M. Cook
United States Navy
15 PUBLICATIONS **172** CITATIONS
SEE PROFILE

Michel Barsoum
Drexel University
450 PUBLICATIONS **14,195** CITATIONS
SEE PROFILE

Yury Gogotsi
Drexel University
627 PUBLICATIONS **26,385** CITATIONS
SEE PROFILE

Journal of Materials Chemistry A

COMMUNICATION

View Article Online
View Journal

Cite this: DOI: 10.1039/c4ta02638a

Dye adsorption and decomposition on two-dimensional titanium carbide in aqueous media†

O. Mashtalir, K. M. Cook, V. N. Mochalin, M. Crowe,‡ M. W. Barsoum and Y. Gogotsi*

Received 26th May 2014
Accepted 17th July 2014

DOI: 10.1039/c4ta02638a

www.rsc.org/MaterialsA

Recently a large family of two-dimensional (2D) layered early transition metal carbides and carbonitrides – labelled MXene – possessing metallic conductivity and hydrophilic surfaces was discovered. Herein we report on the adsorption and photocatalytic decomposition of organic molecules in aqueous environments containing $Ti_3C_2T_x$, a representative of the MXene family. This material possesses excellent adsorption toward cationic dyes, best described by a Freundlich isotherm. We also found that the material may undergo structural changes in aqueous media.

Layered materials have long been a subject of research due to their interesting properties and potential in a variety of technologies. A great deal of effort has been directed toward solving major societal challenges, including energy storage and environmental pollution. In the area of energy storage, layered materials have potential applications in electrochemical capacitors[1] and Li-ion batteries.[2] They are also promising materials for sorption and catalysis in environmental applications.[3] The advantages of layered materials in both types of applications stem from their large and highly-accessible surfaces with controlled chemistries.[4] In the environmental application realm, research is focused on improving their chemical and environmental stabilities, or reusability and recyclability (*e.g.*, recovery of adsorbed oil from exfoliated graphite by compression).[5] Additional work has been performed to render layered materials for specific applications, such as tailoring redox properties, imparting biocompatibility, and improving buoyancy for more efficient utilization of solar radiation, *etc.*[6,7]

Recently, a new family of two-dimensional (2D) early transition metal ternary carbides and carbonitrides – labelled MXenes – was discovered.[8,9] MXenes are produced by etching the A-group element layers from their corresponding MAX phases by hydrofluoric acid, HF.[10–12] HF is a highly selective etchant of silicon carbide capable of distinguishing even between different SiC polytypes.[13] To date, the reported experimental studies have mainly explored the potential of MXenes in electrical energy storage, *e.g.*, electrodes of lithium ion batteries,[14–16] lithium ion capacitors[17] and supercapacitors.[18] However, energy storage is only a small subset of potential applications wherein the unique structures and, more important, diverse chemistries of MXenes may prove beneficial.

MXenes are composed of $M_{n+1}X_n$ stacked sheets – where M is an early transition metal and X is carbon and/or nitrogen – held together by van der Waals interactions and/or hydrogen bonds (see schematic and SEM images in Fig. 1a and b). The surfaces of MXene sheets are typically terminated with OH, O and/or F, resulting in a general formula $M_{n+1}X_nT_x$, where T_x indicates a surface termination and x the number of surface groups per formula unit.[9,18] Computational studies have predicted some $M_{n+1}X_nT_x$ to be narrow band gap semiconductors.[8,16,19,20] that can be tuned by altering their surface chemistries or the arrangements of the surface groups relative to the M atoms.[16,19,20] The tunability of the band structure suggests that MXenes could potentially be used as photocatalysts. In addition, MXenes may demonstrate catalytic properties, known for transition metal carbides.[21]

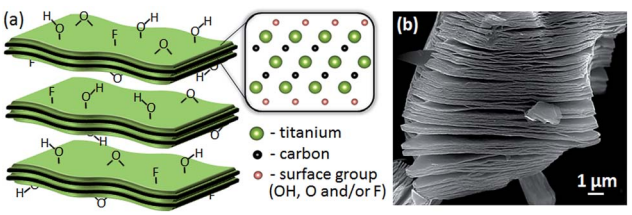

Fig. 1 (a) Schematic of $Ti_3C_2T_x$ layered structure with a side view atomic model of a single sheet. (b) SEM image of a $Ti_3C_2T_x$ particle.

Department of Materials Science & Engineering, A.J. Drexel Nanomaterials Institute, Drexel University, 3141 Chestnut Street, Philadelphia, PA 19104, USA. E-mail: gogotsi@drexel.edu

† Electronic supplementary information (ESI) available: Detailed experimental procedures, additional characterization and discussion. See DOI: 10.1039/c4ta02638a

‡ Permanent address: Chemical Engineering, University of Bath, Claverton Down, Bath, BA2 7AY, UK.

Similar to many other layered materials, MXenes can be intercalated and delaminated into single sheets. Different organic molecules such as hydrazine, urea, dimethyl sulfoxide among others,[15] and a variety of cations, spontaneously intercalate $Ti_3C_2T_x$.[18] This suggests that MXenes could potentially be used as adsorbents, similar to other layered materials.[3] A recent study reported an outstanding sorption capacity of a modified MXene for lead ions.[22] As far as we are aware neither the catalytic properties nor the adsorption of dyes by MXenes have been reported to date.

Herein, we report on our first attempts to use an as-produced multilayered MXene as a potential adsorbent and photocatalyst. For this purpose, we chose to investigate the interaction of $Ti_3C_2T_x$ – to date, the most studied MXene – with the aqueous dyes methylene blue (MB) and acid blue 80 (AB80) in the dark and under ultraviolet (UV) light. The details of $Ti_3C_2T_x$ synthesis and experimental procedures are summarized in the ESI.† We also investigated the structural changes of $Ti_3C_2T_x$ in contact with aqueous MB solutions under different conditions.

In a set of experiments the adsorption kinetics of the dyes onto $Ti_3C_2T_x$ was studied. Since $Ti_3C_2T_x$ was reported to have negatively charged surfaces,[18] we chose to investigate the effects of the adsorptive charge in this process. For this, MB (a cationic dye) and AB80 (an anionic dye) were selected (their chemical structures are shown in insets in Fig. 2a).

Fig. 2a shows the time dependence of the $Ti_3C_2T_x$-mediated removal of each dye from solution in the dark. While, even after 20 h, there were no changes in the AB80 concentration, a dramatic decrease of MB concentration was observed within the first 8 h. From these results, it is reasonable to assume that the preferential adsorption of the cationic dye, MB, over the anionic dye, AB80, in the dark is primarily due to favorable electrostatic interactions between the MB molecules and the MXene surfaces.

Adsorption isotherms of MB on $Ti_3C_2T_x$ are shown in Fig. 2b. Two models, Langmuir and Freundlich, were used to fit the experimental data (details on the models and corresponding equations can be found in the ESI†). The best fitting parameters of both isotherms (Fig. 2b) together with their correlation coefficients are presented in Table 1. High values of K_L, a constant which characterizes the strength of adsorbate binding to the adsorbent (eqn (1), ESI†), suggest that MB binds strongly to $Ti_3C_2T_x$. The separation factor, R_L, calculated from the Langmuir isotherm using eqn (2) (ESI†) was plotted *vs.* initial MB concentrations (inset in Fig. 2b). The R_L values are close to zero (10^{-5} to 10^{-4} for the range of MB concentrations explored), indicating nearly irreversible adsorption.[23] Pearson's correlation coefficient, R, for the Freundlich isotherm is higher than the corresponding value for the Langmuir isotherm (Table 1), meaning that the Freundlich model is an overall better fit of the experimental results (Fig. 2b). The value of the constant ν (eqn (3), ESI†) is larger than 1 which also indicates favorable adsorption in the Freundlich model.[24] The fact that the latter model better describes adsorption is consistent with the presence of heterogeneous adsorption sites on the MXene surfaces, a reasonable conclusion given that, as noted above, the MXenes are primarily terminated by a mix of OH, O and F (see schematic in Fig. 1a).

The adsorption capacity of $Ti_3C_2T_x$ for MB is ~39 mg g^{-1} (Table 1). This value is smaller than typically observed for commercial activated carbons (up to 1000 mg g^{-1})[25] but comparable with other materials of similar structure and surface areas (from ~14 mg g^{-1} for raw kaolinite,[26] up to ~290 mg g^{-1} for commercial montmorillonite clays[27]). This suggests that MXenes, with their tailorable and various compositions and surface chemistries, might be better adsorbents than other 2D materials.

When an aqueous 0.05 mg mL^{-1} MB solution was in contact with suspended $Ti_3C_2T_x$ multilayers in the dark, the MB concentration continued to decrease steadily over a period of days after the initial rapid drop during the first 2 h (Fig. 2a). To better understand the reason for this slow concentration decrease, the $Ti_3C_2T_x$ structure after MB adsorption was studied. According to X-ray diffraction (XRD) analysis of recovered MXene powders (Fig. 3), after the 2 h adsorption in the dark, no changes in the position of the (0002) XRD peak were observed. After the 20 h adsorption, a small shift of that peak towards lower angles was detected. In addition, this peak broadened, suggesting imperfect stacking in the [000l] direction. Because of the ability of cations to intercalate MXenes,[18] and the intercalation of dyes reported for many layered materials,[28,29] the possibility of MB intercalation into $Ti_3C_2T_x$ was considered. According to XRD (Fig. 3) the value of the *c*-lattice parameter (*c*-LP) increased by 2.0 Å. The MB molecule dimensions are ≈ 17.0 × 7.6 × 3.25 $Å^3$ ($l \times w \times h$).[30] Assuming that

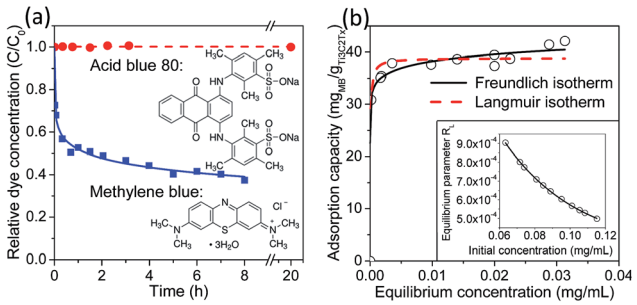

Fig. 2 (a) Time dependence of MB (C_0 = 0.05 mg mL^{-1}) and AB 80 (C_0 = 0.06 mg mL^{-1}) concentrations in aqueous solutions with suspended $Ti_3C_2T_x$ particles in the dark. Chemical structures of corresponding dyes are shown as insets. (b) Adsorption isotherms of MB on $Ti_3C_2T_x$. Inset shows dependence of the equilibrium parameter R_L (see eqn (2), ESI†) on initial concentration, C_0, of MB.

Table 1 Fitting parameters for Langmuir and Freundlich isotherms for MB on $Ti_3C_2T_x$

Langmuir isotherm	Freundlich isotherm
A_{max} = 38.851 mg g^{-1}	ν^b = 19.963
K_L = 1.743 × 104 mL mg^{-1}	$K_F{}^b$ = 48.152
R^a = 0.811	R^a = 0.928

[a] Pearson's correlation coefficient. [b] Values calculated for C expressed in mg mL^{-1} and A in mg g^{-1} (see eqn (3), ESI†).

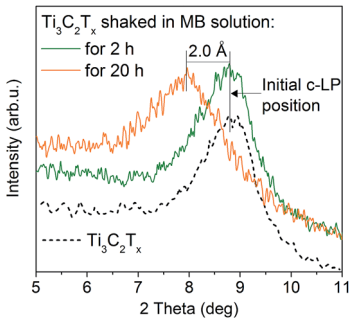

Fig. 3 X-Ray diffraction patterns around the $Ti_3C_2T_x$ (0002) peak before and after soaking in aqueous 0.05 mg mL^{-1} MB solution for 2 h and 20 h.

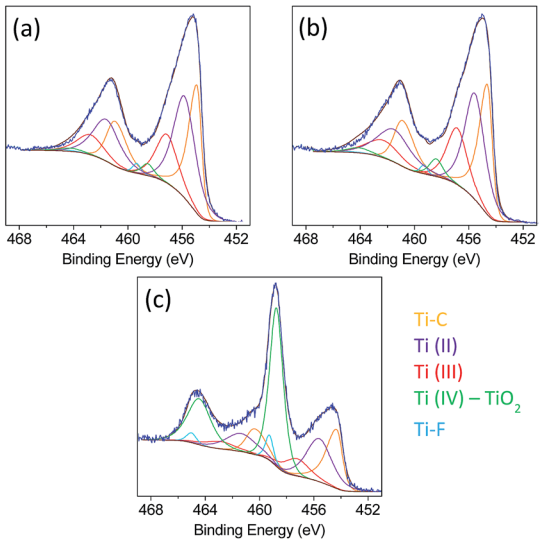

Fig. 4 High-resolution XPS in the Ti 2p region for $Ti_3C_2T_x$, (a) before MB absorption, (b) after 20 h MB adsorption, (c) after 1 week in a 0.05 mg mL^{-1} MB aqueous solution shaken in the dark in aerated conditions. The fits are color-coded; the key is shown on the right of (c). An increase in the Ti $2p_{3/2}$ component corresponding to TiO_2 (colored green) can be observed at 458.8 eV.

one MB molecule intercalates into the interlayer space between the $Ti_3C_2T_x$ sheets in an orientation parallel to the surfaces, the anticipated increase in *c*-LP should be at least 3.25 Å, *i.e.* 1.5 times the observed increase. Thus, the 2 Å increase in the interlayer space of $Ti_3C_2T_x$ is not enough to accommodate a MB molecule. Still, partial wedging-in of MB molecules at the particles' edges, could in principle cause their opening and result in the observed increase of *c*-LP.

As discussed below, $Ti_3C_2T_x$ sheets in aqueous solutions slowly react with water, and transform into titanium hydroxide. This intrinsic instability in water provides an alternative explanation for the observed increase in *c*-LP. This transformation, that initiates at the particle's edges, could again wedge open the layers resulting in broader 0002 peaks. Interestingly, keeping the $Ti_3C_2T_x$ powder in a MB solution for up to 7 days had no further effect on the *c*-LP values. Clearly, more work is needed to better understand the reasons for the shifts in LPs.

To determine if any non-photocatalytic redox processes were occurring on the $Ti_3C_2T_x$ surfaces in aqueous MB solution in the dark, the chemical state of the $Ti_3C_2T_x$ powders – un-sputtered surfaces – was monitored by X-ray photoelectron spectroscopy (XPS) over time. Aliquots of this solution were taken after 2 h and 20 h, from which suspended $Ti_3C_2T_x$ powders were separated by centrifugation for analysis. High-resolution XPS spectra in the Ti 2p region of the powder before contact with the MB solution revealed peaks that could be deconvoluted into components corresponding to Ti bound to C, Ti(II) oxide, Ti(III) oxide and peaks that could be due to Ti(IV) oxide and/or Ti bound to F (Fig. 4a; Table S1†). This spectrum is typical of $Ti_3C_2T_x$, wherein Ti oxides and Ti–F signals are observed, together with Ti–C signals arising from Ti atoms in the interior of the MXene layers.[15,31,32] According to Fig. 4, exposure to the aqueous 0.05 mg mL^{-1} MB solution for up to 20 h does not significantly change the chemical states of the atoms in $Ti_3C_2T_x$ (Fig. 4a and b). Subtle changes in the spectra (*e.g.* a more pronounced shoulder at ~457 eV) as well as an increased contribution from the peak corresponding to Ti(IV) – *viz.* TiO_2 – can be observed after 20 h exposure (Fig. 4b) in comparison to the spectra of $Ti_3C_2T_x$ before contact with aqueous MB (Fig. 4a).

Although the changes to the spectrum in Fig. 4b are slight, after a week exposure, a peak corresponding to TiO_2 became quite clear (Fig. 4c; see also Table S1† for references). Concomitant with the increase in the TiO_2 signal, there was a decrease in the Ti_3C_2 signal. The component assigned to Ti bound to F also shifts significantly to lower binding energy (compare Fig. 4a and c). All these observations indicate that multilayered $Ti_3C_2T_x$ particles slowly react to form titanium hydroxide and/or TiO_2[33] on their surfaces. The slight shift to lower binding energy for the Ti–C component and the slight shift to higher binding energy for the TiO_2 component over the one week period may indicate the initial stages of the separation of these phases as the local effect of removing oxygen from the MXene into the TiO_2 could cause a shift in electron density. Such long-term oxidation is, most probably, a result of the presence of dissolved oxygen in the solution which acts as oxidizer, as predicted theoretically[34] and confirmed experimentally herein. This reaction consumes Ti and C, forming TiO_2 and CO_2. Compelling evidence for the oxidation of $Ti_3C_2T_x$ into various Ti oxides can be found in ESI, Fig. S2 and S3†. The oxidation may occur due to O_2 adsorption on under coordinated Ti atoms in $Ti_3C_2T_x$ following the mechanism reported for bulk TiO_x.[35] However, even without dissolved oxygen, delaminated $Ti_3C_2T_x$ single flakes slowly react with water, in a fashion reminiscent of the reaction of the topmost 5–30 atomic layers in bulk TiC.[36] The conversion of $Ti_3C_2T_x$ layers into nanoscale TiO_2 may lead to an increase in the accessible surface area, which in turn could explain the continued drop in MB concentration in solution observed for prolonged holding times in the dark.

There are other possible explanations for the observed continued drop in the measured dye concentration. For instance, since the product of MB reduction – leukomethylene blue – is colorless,[37] a process of MXene oxidation to TiO_2 by the MB could be involved. There is also a possibility that $Ti_3C_2T_x$ – like other

transition metal carbides, which have been shown to catalyze oxidation of some gases[21] – could catalyze the oxidation of MB by oxygen.

At this juncture it is clear that the reactions and interactions between $Ti_3C_2T_x$, MB, H_2O, and oxygen in aqueous environment are quite complicated, potentially involving many parallel processes. More detailed studies are needed. In particular, more attention must be paid to the instability of $Ti_3C_2T_x$ in aqueous media, which was not taken into consideration in any of the previous studies of this material.

Fig. 5 compares the time dependencies of the relative concentrations of MB and AB80 in water in the presence of $Ti_3C_2T_x$, while exposed to UV irradiation, with those for samples held in the dark. In particular, in the case of AB80 in the presence of $Ti_3C_2T_x$ – where no changes in dye concentration were observed over 20 h in the dark – fast photodegradation occurred under UV light (Fig. 5b). As a result, 5 h irradiation led to a decrease of the solution concentration of AB80 by 62%. Similarly, 81% of the MB was degraded while in contact with suspended $Ti_3C_2T_x$ during UV irradiation over 5 h, whereas only 18% (~4 times less) of MB was removed in the dark (Fig. 5a). Photolysis of the dyes under UV light under the same conditions was negligible, as confirmed by running separate experiments with dye solutions of the same concentrations, containing no $Ti_3C_2T_x$ (see Fig. S4, ESI†).

It is likely that the formation of titanium hydroxide and/or TiO_2 – both known to have distinct photocatalytic activities,[38–41] – on the MXene surfaces contributes to the photocatalytic effect observed with UV illumination. This again implies that the photocatalytic mechanisms in the presence of $Ti_3C_2T_x$ are quite complicated and warrant deeper study. These comments notwithstanding, the metallic character and the electrical conductivity of $Ti_3C_2T_x$ observed in thin film measurements[42] suggest the presence of free electrons in the carbide layer underneath the oxide surface. Therefore, similar to graphene-titania composites, $Ti_3C_2T_x$ supported TiO_2 composites may be a promising material for catalysis, energy conversion and energy storage applications.

Finally, other members of the MXenes family, more probably than not, also possess yet undiscovered abilities to selectively adsorb and degrade different molecules, as well as catalyze different chemical reactions.

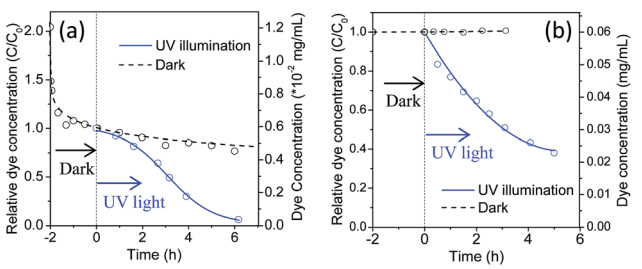

Fig. 5 Time dependence of relative concentrations, C/C_0, of, (a) MB and, (b) AB80 in $Ti_3C_2T_x$ containing solutions. Solid and dashed lines correspond to measurements taken under UV light and in the dark, respectively.

Conclusions

In summary, a representative MXene, multilayered $Ti_3C_2T_x$, was tested for its adsorptive and photocatalytic properties. We show that it is a quite efficient adsorbent for the cationic dye MB. Adsorption of MB on $Ti_3C_2T_x$ was fit by Langmuir and Freundlich isotherms and most closely followed the Freundlich model, with fitting parameters ν and K_F equal to 19.96 and 48.15, respectively. The strength of binding, K_L, determined from the Langmuir equation, implies that the dye is exceptionally strongly, and irreversibly, bonded to the $Ti_3C_2T_x$ surfaces in aqueous solutions.

When $Ti_3C_2T_x$ and aqueous MB are mixed and held in the dark under ambient conditions, three stages have been identified: (1) active adsorption of MB molecules onto $Ti_3C_2T_x$ surfaces during the first 2 h; (2) an increase of stacking disorder, possibly due to wedging of the layered structure and/or chemical MXene transformation in the next 18 h and, (3) oxidation of $Ti_3C_2T_x$ resulting in the formation of titania over long periods of time, especially in the presence of dissolved oxygen.

The limited stability of $Ti_3C_2T_x$ in water has important practical implications. One critical instance is that water is not the best medium to store $Ti_3C_2T_x$ after synthesis. It also has important ramifications – as shown herein – in terms of interpreting our results and understanding MXene chemistry.

We also show, for the first time, that MB and AB80 dye degradation is enhanced when UV light is illuminated on solutions containing both dye and $Ti_3C_2T_x$. The complex processes involved in photodegradation need further studies.

Acknowledgements

We thank M. Naguib and C. E. Ren for providing the $Ti_3C_2T_x$ material, M. Lukatskaya for SEM analysis, B. Dyatkin for BET analysis, and the Centralized Research Facility of Drexel University for access to XRD, SEM and TEM equipment. MXene synthesis was funded by the National Science Foundation (DMR-1310245). Photocatalytic work was supported by the Fluid Interface Reactions, Structure and Transport (FIRST) Center, an Energy Frontier Research Center funded by the US Department of Energy, Office of Basic Energy Studies.

Notes and references

1 M. D. Stoller, S. Park, Y. Zhu, J. An and R. S. Ruoff, *Nano Lett.*, 2008, **8**, 3498–3502.
2 M. A. Bizeto, A. L. Shiguihara and V. R. L. Constantino, *J. Mater. Chem.*, 2009, **19**, 2512–2525.
3 S. M. Auerbach, K. A. Carrado and P. K. Dutta, *Handbook of Layered Materials*, CRC Press, New York, NY, USA, 2004.
4 Y. Gogotsi, *J. Phys. Chem. Lett.*, 2011, **2**, 2509–2510.
5 M. Toyoda and M. Inagaki, *Carbon*, 2000, **38**, 199–210.
6 M. V. Savoskin, A. P. Yaroshenko, N. I. Lazareva, V. N. Mochalin and R. D. Mysyk, *J. Phys. Chem. Solids*, 2006, **67**, 1205–1207.
7 Y. X. Xu and G. Q. Shi, *J. Mater. Chem.*, 2011, **21**, 3311–3323.

8 M. Naguib, M. Kurtoglu, V. Presser, J. Lu, J. J. Niu, M. Heon, L. Hultman, Y. Gogotsi and M. W. Barsoum, *Adv. Mater.*, 2011, **23**, 4248–4253.
9 M. Naguib, V. N. Mochalin, M. W. Barsoum and Y. Gogotsi, *Adv. Mater.*, 2014, **26**, 992–1005.
10 M. Naguib, O. Mashtalir, J. Carle, V. Presser, J. Lu, L. Hultman, Y. Gogotsi and M. W. Barsoum, *ACS Nano*, 2012, **6**, 1322–1331.
11 O. Mashtalir, M. Naguib, B. Dyatkin, Y. Gogotsi and M. W. Barsoum, *Mater. Chem. Phys.*, 2013, **139**, 147–152.
12 M. Naguib, J. Halim, J. Lu, K. M. Cook, L. Hultman, Y. Gogotsi and M. W. Barsoum, *J. Am. Chem. Soc.*, 2013, **135**, 15966–15969.
13 Z. G. Cambaz, G. N. Yushin, Y. Gogotsi and V. G. Lutsenko, *Nano Lett.*, 2006, **6**, 548–551.
14 M. Naguib, J. Come, B. Dyatkin, V. Presser, P. L. Taberna, P. Simon, M. W. Barsoum and Y. Gogotsi, *Electrochem. Commun.*, 2012, **16**, 61–64.
15 O. Mashtalir, M. Naguib, V. N. Mochalin, Y. Dall'Agnese, M. Heon, M. W. Barsoum and Y. Gogotsi, *Nat. Commun.*, 2013, **4**, 1716.
16 Q. Tang, Z. Zhou and P. W. Shen, *J. Am. Chem. Soc.*, 2012, **134**, 16909–16916.
17 J. Come, M. Naguib, P. Rozier, M. W. Barsoum, Y. Gogotsi, P. L. Taberna, M. Morcrette and P. Simon, *J. Electrochem. Soc.*, 2012, **159**, A1368–A1373.
18 M. R. Lukatskaya, O. Mashtalir, C. E. Ren, Y. Dall'Agnese, P. Rozier, P. L. Taberna, M. Naguib, P. Simon, M. W. Barsoum and Y. Gogotsi, *Science*, 2013, **341**, 1502–1505.
19 A. N. Enyashin and A. L. Ivanovskii, *Comput. Theor. Chem.*, 2012, **989**, 27–32.
20 M. Khazaei, M. Arai, T. Sasaki, C. Y. Chung, N. S. Venkataramanan, M. Estili, Y. Sakka and Y. Kawazoe, *Adv.Funct. Mater.*, 2013, **23**, 2185–2192.
21 N. I. Ilchenko and Y. I. Pyatnitsky, in *The Chemistry of Transition Metal Carbides and Nitrides*, ed. S. T. Oyama, Springer, Netherlands, 1996, pp. 311–326.
22 Q. M. Peng, J. X. Guo, Q. R. Zhang, J. Y. Xiang, B. Z. Liu, A. G. Zhou, R. P. Liu and Y. J. Tian, *J. Am. Chem. Soc.*, 2014, **136**, 4113–4116.
23 K. R. Hall, L. C. Eagleton, A. Acrivos and T. Vermeulen, *Ind. Eng. Chem. Fundam.*, 1966, **5**, 212–223.
24 H. Freundlich, *Colloid & Capillary Chemistry*, E.P. Dutton & Co, New York, NY, USA, 1922.
25 M. Rafatullah, O. Sulaiman, R. Hashim and A. Ahmad, *J. Hazard. Mater.*, 2010, **177**, 70–80.
26 D. Ghosh and K. G. Bhattacharyya, *Appl. Clay Sci.*, 2002, **20**, 295–300.
27 C. A. P. Almeida, N. A. Debacher, A. J. Downs, L. Cottet and C. A. D. Mello, *J. Colloid Interface Sci.*, 2009, **332**, 46–53.
28 P. Bradder, S. K. Ling, S. B. Wang and S. M. Liu, *J. Chem. Eng. Data*, 2011, **56**, 138–141.
29 P. Liu and L. X. Zhang, *Sep. Purif. Technol.*, 2007, **58**, 32–39.
30 P. T. Hang and G. W. Brindley, *Clays Clay Miner.*, 1970, **18**, 203–212.
31 O. Wilhelmsson, J. P. Palmquist, E. Lewin, J. Emmerlich, P. Eklund, P. O. A. Persson, H. Hogberg, S. Li, R. Ahuja, O. Eriksson, L. Hultman and U. Jansson, *J. Cryst. Growth*, 2006, **291**, 290–300.
32 S. Myhra, J. A. A. Crossley and M. W. Barsoum, *J. Phys. Chem. Solids*, 2001, **62**, 811–817.
33 S. Yamamoto, H. Bluhm, K. Andersson, G. Ketteler, H. Ogasawara, M. Salmeron and A. Nilsson, *J. Phys.: Condens. Matter*, 2008, **20**(184025), 1–14.
34 L. Y. Gan, D. Huang and U. Schwingenschlogl, *J. Mater. Chem. A*, 2013, **1**, 13672–13678.
35 E. Lira, S. Wendt, P. P. Huo, J. O. Hansen, R. Streber, S. Porsgaard, Y. Y. Wei, R. Bechstein, E. Laegsgaard and F. Besenbacher, *J. Am. Chem. Soc.*, 2011, **133**, 6529–6532.
36 A. I. Avgustinik, G. V. Drozdetskaya and S. S. Ordan'yan, *Powder Metall. Met. Ceram.*, 1967, **6**, 470–473.
37 S. Mowry and P. J. Ogren, *J. Chem. Educ.*, 1999, **76**, 970–974.
38 K. Nakata and A. Fujishima, *J. Photochem. Photobiol., C*, 2012, **13**, 169–189.
39 A. Houas, H. Lachheb, M. Ksibi, E. Elaloui, C. Guillard and J. M. Herrmann, *Appl. Catal., B*, 2001, **31**, 145–157.
40 T. A. Stewart, M. Nyman and M. P. deBoer, *Appl. Catal., B*, 2011, **105**, 69–76.
41 D. Q. Zhang, G. S. Li and J. C. Yu, *J. Mater. Chem.*, 2010, **20**, 4529–4536.
42 J. Halim, M. R. Lukatskaya, K. M. Cook, J. Lu, C. R. Smith, L.-Å. Näslund, S. J. May, L. Hultman, Y. Gogotsi, P. Eklund and M. W. Barsoum, *Chem. Mater.*, 2014, **26**, 2374–2381.